1983

Gravity-induced density and concentration profiles in binary mixtures near gas–liquid critical lines

R. F. Chang
National Bureau of Standards

J. M. H. Levelt Sengers
National Bureau of Standards

T. Doiron
Virginia Commonwealth University

J. Jones
Virginia Commonwealth University

Chang, R. F., Levelt Sengers, J. M. H., & Doiron, T., et al. Gravity-induced density and concentration profiles in binary mixtures near gas–liquid critical lines. The Journal of Chemical Physics, 79, 3058 (1983).

Gravity-induced density and concentration profiles in binary mixtures near gas–liquid critical lines

R. F. Chang and J. M. H. Levelt Sengers

Thermophysics Division, National Bureau of Standards, Washington, D.C. 20234

T. Doiron[a] and J. Jones

Physics Department, Virginia Commonwealth University, Richmond, Virginia 23284
(Received 12 April 1983; accepted 17 June 1983)

We have calculated gravity-induced density and concentration gradients using scaled equations of state fashioned after that of Leung and Griffiths for binary mixtures near gas–liquid critical lines. The mixtures considered here are those of helium-3 and helium-4 and of carbon dioxide and ethane. Our calculations show that the density profiles for both mixtures in any proportion of the components are similar to those of pure fluids. The concentration gradients in the helium mixture have the same appearance as the density gradients. In the carbon dioxide–ethane system, however, the form of the concentration profile varies greatly, depending on the overall composition. Moreover, the temperature at which a mixture separates into two phases is slightly different from that expected for the mixture in the absence of gravity. We have also examined the case where a mixture is subjected to a large gravitational field such as can be generated in a centrifuge and found that, although the density gradient in all the mixtures is like that in pure fluids, the concentration gradients in the mixtures of carbon dioxide and ethane have complex features related to the presence of critical azeotropy.

I. INTRODUCTION

At a critical point, a system is only marginally stable and certain second derivatives of the thermodynamic free energy diverge. Thus, in simple fluids the isothermal compressibility diverges and consequently, as Gouy pointed out[1] as early as 1892, large density gradients will be induced by the gravitational field in a near-critical fluid. Similarly, in a binary liquid mixture near a consolute point, the osmotic susceptibility diverges and gravity induces substantial concentration gradients.

Because of the nonuniformity of the states in the sample cell, the measurement of bulk thermodynamic properties such as the specific heat near a critical point will be affected. The errors introduced by the gravitational stratification can be evaluated by means of the scaling laws.[2,3] Experiments using light-scattering techniques will also be affected because physical properties such as refractive index and turbidity will vary with height.[4–8] On the other hand, the gravity-induced density and concentration gradients contain information on the equation of state of the system near a critical point; use has been made of this fact in several experiments in pure fluids[9,10] and in binary liquid mixtures.[11–15] The effects of high gravitational fields have also been measured in binary liquid mixtures.[15,16]

The experimental exploitation of gravity effects in binary mixtures near a gas–liquid critical point (also known as a plait point) was begun only recently by Meyer and co-workers,[17] although the first theoretical description of the separation of phases in a binary mixture near a plait point in the field of gravity was presented by Kuenen in 1895.[18] In such mixtures, both density and concentration gradients may be present.

In the case of a simple fluid, if a cell is filled at an average density $\langle\rho\rangle$ (henceforth referred to as the bulk density) close to and including the critical density ρ_c, the critical density will actually be attained at only one particular level in the cell. Similarly, in a binary liquid mixture the critical concentration x_c will prevail at only one particular level. In both cases, this particular level is where the meniscus first appears as the sample is cooled to below the critical temperature. The density profile in a simple fluid and the concentration profile in a binary liquid mixture are, to a good approximation, antisymmetric with respect to this level. Therefore, if the cell is filled with a pure fluid at $\langle\rho\rangle$ equal to ρ_c or with a binary liquid at $\langle x\rangle = x_c$ the meniscus will first appear at the center of the cell. (The sample cell is always assumed to have cross sections uniform along the height.)

In the case of a binary mixture near a plait point, a sample is characterized by two parameters: the bulk number density $\langle\rho\rangle$, and the bulk concentration $\langle x\rangle$ which is defined as the bulk number density of component 1 divided by $\langle\rho\rangle$. Suppose the sample is prepared such that the combination of $\langle\rho\rangle$ and $\langle x\rangle$ corresponds to a state on the critical line with the associated critical temperature T_c. In the field of gravity one cannot, as in the case of a pure fluid system, expect the meniscus in the mixture to appear first at temperature T_c, because at this temperature the state characterized by $\langle\rho\rangle$ and $\langle x\rangle$ may not be realized at any level in the cell. If at some level z in the cell, a state, characterized by ρ' and x' and corresponding to a different point on the critical line, is realized at T_c', then the system will separate into two phases at T_c' and the meniscus will form at z. Nor can one take for granted that the meniscus of the sample characterized by $\langle\rho\rangle$ and $\langle x\rangle$ on the critical line will form in the center of the cell.

The calculation of the gravity effects in binary mix-

[a]Present address: Automated Production Technology Division, National Bureau of Standards, Washington, D.C. 20234.

 0021-9606/83/183058-09$02.10

tures near a gas–liquid critical point was motivated by two light-scattering experiments. The first experiment is in the mixture of carbon dioxide and ethane[19] and the other is in the mixture of helium-3 and helium-4.[20] In both experiments, bending of the light beam passing through the sample has been observed just like in a pure fluid system. Moreover, in the experiment of mixtures of He^3 and He^4, Miura *et al.*[20] have also reported that the meniscus first appeared at a temperature above the critical temperature of the bulk sample and at a level below the center of the cell. As the temperature decreased further, the meniscus first rose to a maximum level and then fell back to settle at the center of the cell. Our purpose is to investigate whether these phenomena can be ascribed to the effect of gravity. For this task, previous investigations of gravity effects in mixtures near a gas–liquid critical point, such as Mistura's derivation of the power law behavior of the change of concentration and density with height,[21] and the studies of sedimentation by Malyshenko and Mika[22] proved to be insufficient. For our purpose, a complete scaled equation of state of a mixture near a plait point is required. Such an equation has been developed by Leung and Griffiths for mixtures of helium-3 and helium-4.[23] Their equation of state is derived from a thermodynamic potential based on the idea that the concept of critical-point universality and the scaling hypothesis are applicable to mixtures when a suitable set of variables is used. The properties of a binary mixture are then predictable from an interpolation between the critical properties of individual pure components.

For the mixture of carbon dioxide and ethane we have adopted an equation of state[24] fashioned after that of Leung and Griffiths. By the use of this equation one can calculate and examine the behavior of a mixture near a gas–liquid critical point. These two choices of mixtures form an interesting contrast because on the one hand the critical temperatures of He^3 and He^4 are far apart, their ratio being about 0.6, while on the other hand the mixture of CO_2 and C_2H_6, with less than 1% difference in critical temperatures, exhibits critical azeotropy.

In Sec. II, we present the equation of state, and in Sec. III we introduce the dependence of the thermodynamic properties on the height z as a consequence of the gravitational field. Density and concentration profiles calculated for mixtures of helium-3 and helium-4 and of carbon dioxide and ethane, for various concentrations and temperatures, are presented in Sec. IV and discussed in Sec. V. Profiles are also calculated in high gravitational fields. A short critique is presented in Sec. VI while Sec. VII summarizes our principal results and conclusions.

II. THE EQUATION OF STATE

We refer readers to Ref. 23 for a detailed description of the Leung–Griffiths equation of state for near-critical mixtures. Here we shall present the equation of state of mixtures in a general form which contains a few more terms than that of Ref. 23 to accommodate both the mixtures of He^3 and He^4 and of CO_2 and C_2H_6. Original notations from Ref. 23 are retained except that the original subscripts 3 and 4 referring to He^3 and He^4, respectively, are replaced by subscripts 1 and 2, respectively, referring to components 1 and 2.

The basic equation is the thermodynamic potential ω which is chosen to be the pressure p divided by RT, where R is the gas constant and T is the absolute temperature

$$\omega(\zeta, \tau, h) = p/RT \ . \tag{1}$$

The independent variables, ζ, τ, and h, are related to T and the molar chemical potentials μ_1 and μ_2 in the following way:

$$\zeta = C_2 \exp(\mu_2/RT)/\Theta \ , \tag{2}$$

$$\tau = B_c(\zeta) - B \ , \tag{3}$$

$$h = \ln\Theta - H(\zeta, \tau) \ , \tag{4}$$

where

$$\Theta = C_1 \exp(\mu_1/RT) + C_2 \exp(\mu_2/RT) \ , \tag{5}$$

$$B = 1/RT \ , \tag{6}$$

$$B_c(\zeta) = a_0 + a_1\zeta + a_2\zeta(1-\zeta) + a_3\zeta^2(1-\zeta) \ , \tag{7}$$

$$H(\zeta, \tau) = b_1\zeta + b_2\zeta^2 + g_1\zeta\tau + s(\zeta)\tau^2 \ , \tag{8}$$

with

$$s(\zeta) = s_0 + s_1\zeta + s_2\zeta(1-\zeta) \ . \tag{9}$$

Furthermore, the potential ω is written in two parts:

$$\omega = \omega_r(\zeta, \tau, h) + \omega_s(\zeta, \tau, h) \ , \tag{10}$$

where ω_r is the "regular" part and ω_s is the "singular" part which incorporates the critical anomalies. The regular part is assumed to be a polynomial in ζ, τ, and h

$$\omega_r = c(\zeta) + d(\zeta)\tau + e(\zeta)\tau^2 + f(\zeta)h \ , \tag{11}$$

where

$$c(\zeta) = c_0 + c_1\zeta + c_2\zeta(1-\zeta) + c_3\zeta^2(1-\zeta) \ , \tag{12}$$

$$d(\zeta) = d_0 + d_1\zeta \ , \tag{13}$$

$$e(\zeta) = e_0 + e_1\zeta \ , \tag{14}$$

and

$$f(\zeta) = f_0 + f_1\zeta + f_2\zeta(1-\zeta) \ . \tag{15}$$

The singular part takes on the form

$$\omega_s = q(\zeta)\pi(\bar{\tau}, h) \ , \tag{16}$$

with

$$\bar{\tau} = l(\zeta)\tau \ , \tag{17}$$

where

$$q(\zeta) = 1 + q_1\zeta + q_2\zeta(1-\zeta) \ , \tag{18}$$

$$l(\zeta) = 1 + l_1\zeta \ , \tag{19}$$

and $\pi(\bar{\tau}, h)$ is the Schofield "linear model"[25] which is given in a parametric form

$$\pi(\bar{\tau}, h) = r^{2-\alpha}\bar{p}(\theta) \ ; \tag{20}$$

with

TABLE I. Constants in the equation of state of the mixtures.

Constants	He^3+He^4	$CO_2+C_2H_6$	Constants	He^3+He^4	$CO_2+C_2H_6$
T_{c1} K	3.3105	304.133	f_1 mol/m^3	3480	−3747
a_0 mol/J	3.633×10^{-2}	3.9546×10^{-4}	f_2 mol/m^3	500	−4300
a_1 mol/J	-1.315×10^{-2}	-1.549×10^{-6}	g_1 J/mol	39.1	4053
a_2 mol/J	0	1.056×10^{-4}	l_1	0.844	−0.03
a_3 mol/J	0	-7.5006×10^{-5}	q_1	0.32	−0.37
b_1	0.25	−0.3	q_2	−0.25	−0.80
b_2	0.2568	−0.15	s_0 (J/mol)^2	0	-2.772×10^{7}
c_0 mol/m^3	4168	2930	s_1 (J/mol)^2	0	-1.4373×10^{7}
c_1 mol/m^3	1101	−1015	s_2 (J/mol)^2	0	-5.1333×10^{7}
c_2 mol/m^3	100	−550	$\bar{a}$	1.325	5.846
c_3 mol/m^3	300	0	$\bar{g}$ mol/m^3	12 960	15 300
d_0 J/m^3	2.746×10^{5}	4.205×10^{7}	α	0.098	0.1
d_1 J/m^3	3.899×10^{5}	-1.8441×10^{7}	β	0.361	0.355
e_0 J^2/mol-m^3	0	-3.4907×10^{11}	γ	1.18	1.19
e_1 J^2/mol-m^3	0	$1.026\,67\times10^{11}$	δ	4.269	4.352
f_0 mol/m^3	13 820	10 630	Δ	1.541	1.545

$$h=\bar{a}r^{\Delta}\theta(1-\theta^2)\ , \tag{21}$$

and

$$\bar{\tau}=r(1-\bar{b}^2\theta^2)/RT_{c1}\ , \tag{22}$$

where T_{c1} is the critical temperature of the first component, and

$$\bar{b}^2=(\delta-3)/(\delta-1)(1-2\beta)\ . \tag{23}$$

The critical indices α, β, δ, and $\Delta=\beta\delta$ are in their customary notations. The function $\bar{p}(\theta)$ is a polynomial quadratic in θ; it can be found in Ref. 23. The variable r is a measure of the distance of a state from criticality and θ measures the distance along a contour of constant r. The singular behavior at a critical point is then determined by the behavior as $r\to0$.

The equations used for calculating density and concentration profiles are

$$\rho_1=(1-\zeta)\rho-\zeta(1-\zeta)Q\ , \tag{24}$$

$$\rho_2=\zeta\rho+\zeta(1-\zeta)Q\ , \tag{25}$$

$$\rho=\rho_1+\rho_2=\omega_h\ , \tag{26}$$

$$x=\rho_1/\rho\ , \tag{27}$$

and

$$Q=\omega_\zeta+B_\zeta\omega_\tau-\rho(H_\zeta+B_\zeta H_\tau)\ , \tag{28}$$

where the subscripts ζ, τ, and h for ω, B, and H denote partial derivatives with respect to that variable while holding the other two constant. However, B_ζ is the derivative of $B_c(\zeta)$ with respect to ζ. The densities denoted by ρ's are number densities and x, as defined in Eq. (27), is the mole fraction of the first component and is referred to as the concentration in our terminology.

The partial derivatives of ω involve partial derivatives of the Schofield linear model. The explicit expressions for these derivatives can also be found in Ref. 23.

The subscripted coefficients a_0, a_1, a_2, ..., etc. are system-dependent parameters. The values of the coefficients needed in our calculations are listed in Table I for each of the two mixtures.

The values for the critical exponents α, β, γ, δ, and Δ in Table I are not the universal Ising values. We have adopted the "apparent" exponent values instead of the Ising values because, in simple fluids, the truly asymptotic scaled form of the equation of state with Ising exponents is valid only in a very small temperature range close to a critical point.[10] The use of the apparent values, however, allows one to extend the range of temperature in which the scaled equation of state can still be adequately applied to a system.[26]

III. GRAVITY EFFECT

The gravitational field affects the molar chemical potentials μ_1 and μ_2 in an isothermal system in the following way:

$$d\mu_i=-M_i g dz\ ,\quad \text{for } i=1 \text{ and } 2\ , \tag{29}$$

where M_i is the molecular weight of the ith component. By integrating Eq. (29) one obtains

$$\mu_i=\mu_{i0}-M_i gz\ ,\quad \text{for } i=1 \text{ and } 2\ , \tag{30}$$

where μ_{10} and μ_{20} are the constants of integration. The boundary conditions that determine the two constants are the bulk density and the bulk concentration of the sample. The independent variables ζ, τ, and h must now be expressed in terms of z. By combining Eq. (30) with Eqs. (2), (4), and (5) and converting the constants of integration to a more convenient form we obtain

$$\zeta = \zeta_0 / \{(1-\zeta_0)\exp[(m_2-m_1)z]+\zeta_0\}\ , \tag{31}$$

$$h = h_0 + H(\zeta_0,\tau_0) - H(\zeta,\tau) + \ln(\zeta_0/\zeta) - m_2 z\ , \tag{32}$$

where

$$m_i \equiv M_i g/RT\ ,\quad \text{for } i=1 \text{ and } 2\ , \tag{33}$$

and ζ_0, τ_0, and h_0 are the values of ζ, τ, and h, respectively, at $z=0$ which, for convenience, is defined as the center of the cell. In this new form, the two constants of integration are ζ_0 and h_0. The bulk density of a mixture is more sensitive to the value of h_0, whereas the bulk concentration is more sensitive to ζ_0 and thus ζ_0 and h_0 are more practical to use than μ_{10} and μ_{20}. The dependence of τ on z is through ζ only.

By combining Eqs. (31), (32), and (3) with Eqs. (24)–(28) one can calculate the density and concentration profiles for any given values of ζ_0, h_0, and T. However, for a given mixture of known $\langle\rho\rangle$ and $\langle x\rangle$, one must invert an equation such as

$$\langle\rho_i\rangle = \int \rho_i(z,\zeta_0,h_0)dz\ ,\quad \text{for } i=1 \text{ and } 2\ , \tag{34}$$

to express ζ_0 and h_0 in terms of $\langle\rho\rangle$ and $\langle x\rangle$. Such an inversion cannot be carried out analytically. We have found it convenient to determine the profiles from some starting values of ζ_0 and h_0; these parameters are then varied until Eq. (34) is satisfied.

IV. RESULTS

For the calculations of the density and concentration profiles, we choose the bulk parameters of the mixture samples to be those corresponding to a point on a critical line. In other words, for a chosen value of bulk concentration the density will be the critical density determined by the critical line predicted by the equation of state. We have also chosen the height of the sample cell to be 4 mm which is close to that used by Miura *et al.*[20]

As a typical example, density and concentration profiles of a mixture of He^3 and He^4 are calculated as a function of temperature for $\langle x\rangle \simeq 0.69$ which is within the range of concentrations studied by Miura *et al.*[20] The profiles at three different temperatures are shown in Fig. 1. The temperatures expressed in the reduced units, $t=(T-T_c)/T_c$, are, respectively, 1×10^{-4}, -1.4×10^{-5}, and -1×10^{-4} for Figs. 1(a), 1(b), and 1(c). Figure 1(b) shows the profiles of a sample which is at the lowest temperature, within seven-digit resolution, at which the system is still supercritical even though $t<0$. The gravity effect clearly lowered the temperature at which a closed system of given bulk parameters separates into two phases, contrary to the observation of Miura *et al.* that the meniscus formed at a temperature higher than T_c. The shift is caused by the fact that the combination of the bulk density and the bulk concentration is not realized anywhere in the cell. Instead, another point on the critical line with a lower critical temperature is realized at the center of the cell where the meniscus first appears when the system separates into two phases as illustrated in Fig. 1(c). Lowering the temperature further does not move the position of the meniscus in any significant way.

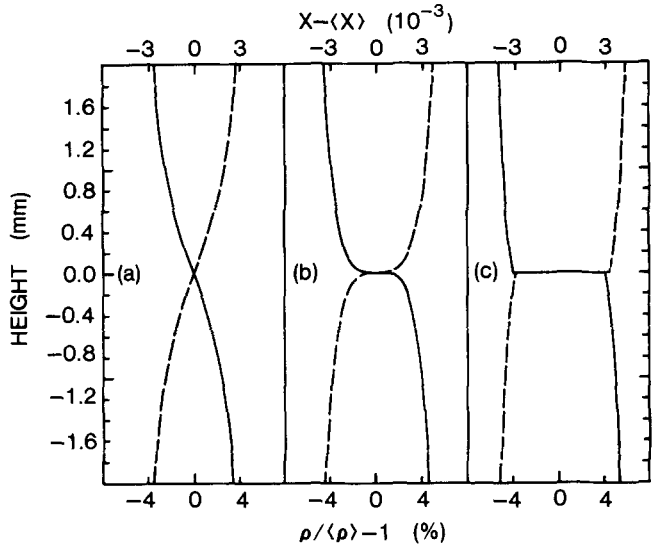

FIG. 1. Gravity-induced density and concentration profiles for a mixture of He^3 and He^4 ($\langle x\rangle = 0.69$) at three temperatures. The solid lines are the density profiles using the bottom scale and the dashed lines are the concentration profiles using the top scale. The temperatures are, $t=1\times10^{-4}$, -1.4×10^{-5}, and -1×10^{-4} for (a), (b), and (c), respectively.

The density and the concentration at the center of the cell near a critical point deviate from $\langle\rho\rangle$ and $\langle x\rangle$ by a very small amount. For instance, in the case of Fig. 1(b), the deviations are on the order of a few parts in 10^5. However, this small effect can be amplified when the height of the cell, or equivalently the gravitational acceleration, is increased as will be discussed further in the next section.

The result of the calculations based on the Leung–Griffiths equation of state of the mixture of He^3 and He^4 does not show the type of meniscus motion observed by Miura *et al.* If we assume that this equation is realistic, we must attribute the observed meniscus motion to some causes other than, or in addition to, the effect of gravity.

One also notices in Fig. 1 that the variation in concentration is about ten times smaller than that in density. This is because the density gradients of both components He^3 and He^4 are close in magnitude and the concentration involves the ratio of two densities. Consequently, the variations in densities cancel to some extent, reducing the variation in the concentration. In other words, even though the critical temperatures of He^3 and He^4 are far apart, the concentrations in coexisting phases are not very different, and neither are the concentration variations induced by gravity.

The density and concentration profiles of a mixture of CO_2 and C_2H_6 calculated for $\langle x\rangle \simeq 0.36$ at three temperatures are shown in Fig. 2. The temperatures are, in reduced units of t, 1×10^{-5}, -7×10^{-8}, and -1×10^{-5}, respectively, for Figs. 2(a)–2(c). In Fig. 2(b) the system is at the lowest temperature, within seven-digit resolution, at which it is still supercritical. By comparing Fig. 1 to Fig. 2, one sees that the effect of gravity on the density is much larger for the mixture of He^3 and He^4 than for that of CO_2 and C_2H_6. The tempera-

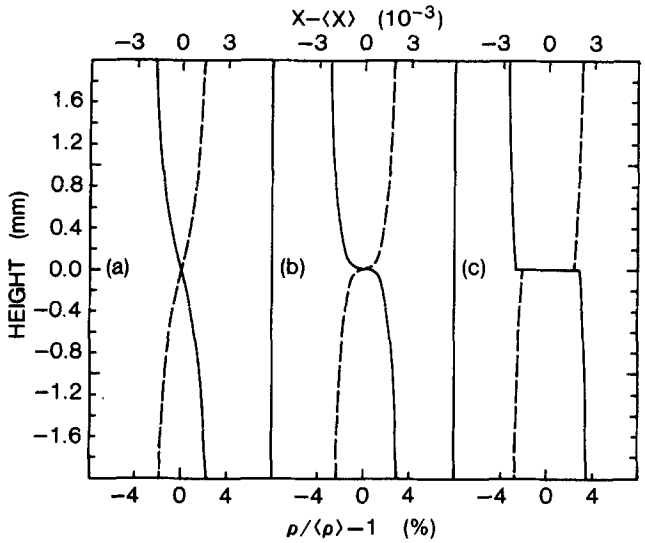

FIG. 2. Gravity-induced density and concentration profiles for a mixture of CO_2 and C_2H_6 ($\langle x\rangle = 0.36$) at three temperatures. The solid lines are the density profiles using the bottom scale and the dashed lines are the concentration profiles using the top scale. The temperatures are, $t = 1\times10^{-5}$, -7×10^{-8}, and -1×10^{-5} for (a), (b), and (c), respectively.

tures have to be ten times closer to T_c for the latter to yield the density profiles that are comparable in size with those of the former. From Eqs. (31) and (33) one sees that $\Delta m \equiv (m_2 - m_1) = (M_2 - M_1)g/RT$ is a measure of the sensitivity of a mixture to the gravitational force. The values of Δm for the mixture of He^3 and He^4 and of CO_2 and C_2H_6 are, respectively, approximately 2.6×10^{-4} m^{-1} and 5.4×10^{-5} m^{-1} near their respective critical lines.

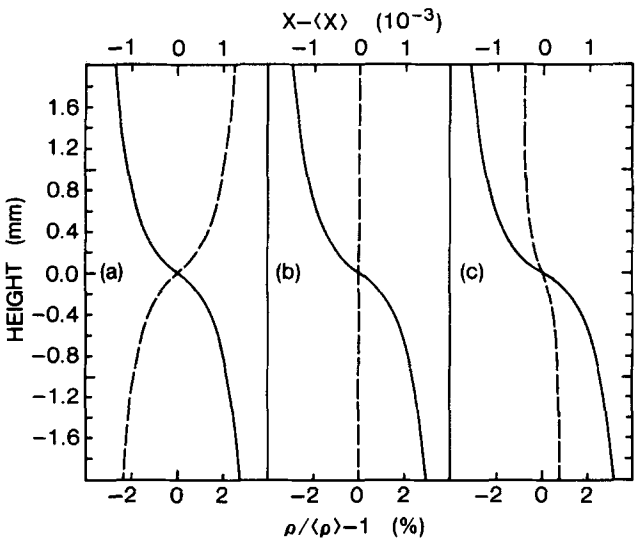

FIG. 3. Gravity-induced density and concentration profiles for a mixture of CO_2 and C_2H_6 at three concentrations near the critical line ($t \simeq 5\times10^{-6}$). The solid lines are the density profiles using the bottom scale and dashed lines are the concentration using the top scale. The concentrations are $\langle x\rangle = 0.50$, 0.72, and 0.84 for (a), (b), and (c), respectively.

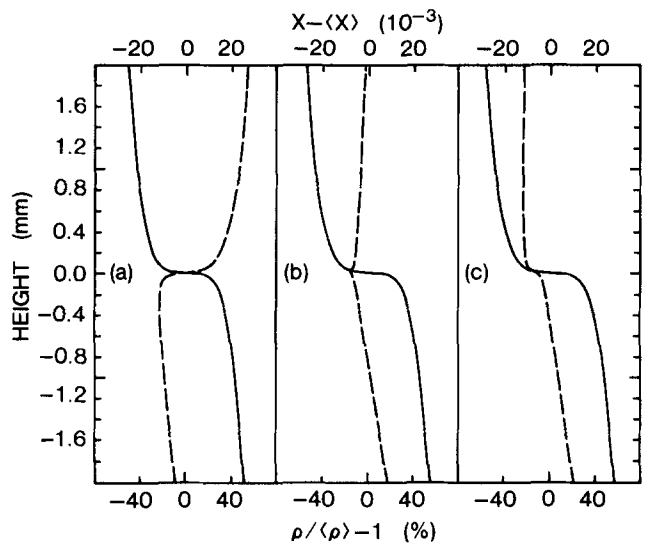

FIG. 4. Density and concentration profiles at $t \simeq 5\times10^{-5}$ for the same mixtures as in Fig. 3 when the gravitational acceleration is increased by a factor of 2×10^5. $X = 1$ represents pure CO_2.

Note also in Fig. 2 that the mixture of CO_2 and C_2H_6 for this concentration is richer in the heavier component CO_2 at the top of the cell. In fact, the mixtures of CO_2 and C_2H_6 show an interesting inversion of the concentration profile on the two sides of the azeotrope, as shown in Fig. 3. The profiles are calculated for concentrations equal to 0.50, 0.72, and 0.84, respectively, for Figs. 3(a)–3(c) and for $t \simeq 5\times10^{-6}$ for all three concentrations. The concentration of the critical azeotrope predicted by the equation of state is about 0.72 ($\langle x\rangle_{caz} \simeq 0.72$). One observes that the density profiles for the mixtures at all three bulk concentrations are virtually identical whereas the concentration profiles are quite different. For $\langle x\rangle = 0.50$ the concentration of CO_2 monotonically increases with increasing height, but for $\langle x\rangle = 0.84$ it decreases instead. At the critical azeotrope ($\langle x\rangle = \langle x\rangle_{caz} = 0.72$) the concentration gradient virtually vanishes, as one expects.

The effects of gravity in a mixture can be amplified by increasing the gravitational acceleration (as can be done in a centrifuge) or equivalently by observing a very tall cell. Therefore, we have also calculated the density and concentration profiles for the same three bulk concentrations as those in Fig. 3, but at $t \simeq 5\times10^{-5}$, when the gravitational acceleration is increased by a factor of 2×10^5. The results of the calculation are shown in Fig. 4. The density profiles for all three concentrations are, again, remarkably alike whereas the concentration profiles are rather distinct. For $\langle x\rangle = 0.50$, shown in Fig. 4(a), the upper half of the concentration profile shows no unusual departure from that in the ordinary gravitational field except for a larger variation in concentration. But most of the lower half of the profile shows that the CO_2 concentration increases with decreasing height, reversing its original trend. The reversal occurs at a level slightly below the center of the cell. For $\langle x\rangle = 0.84$, shown in Fig. 4(c), the CO_2 concentration decreases with increasing height as in the case of the ordinary gravitational field, except for the

region where z is greater than roughly 1 mm. The reversal of the trend makes the profile look rather straight for the upper half of the cell. The most interesting feature is demonstrated by the azeotropic mixture, shown in Fig. 4(b), in which the reversal occurs near the center of the cell resulting in an increase of CO_2 concentration in both upward and downward directions.

V. DISCUSSION

Implicit in the Schofield linear model is the assumption that the densities along the coexistence curve of a pure fluid are symmetric with respect to ρ_c. This assumption leads to an antisymmetric density profile for the gravity effect in simple fluids near a critical point. But the use of this same model in a mixture does not lead to antisymmetric density profiles for each of the two components. The symmetry is broken because ζ varies along z; the symmetry in the model is preserved mathematically only if ζ is held constant. Without the symmetry, the density and the concentration at the center of a cell are different from the bulk (average) values. Nowhere in the cell can one find a level where the density and the concentration match the bulk density and the bulk concentration simultaneously. The broken symmetry leads to a shift in the transition temperature in a mixture. But one must also keep in mind that the deviations from symmetry are rather small. For instance, for the mixture of He^3 and He^4, even when the gravitational acceleration is increased by a factor of 10^4, the transition temperature shifted downwards only by about 13 mK. The density and the concentration at the center of the cell depart, under the same condition of increased gravitational force, from the bulk values by about 8.6% and 0.1%, respectively, at a temperature within 1 μK of the transition temperature and the meniscus forms about 3 μm above the center when the mixture separates into two phases.

The most striking feature emerging from the calculations is the behavior of the concentration profiles for the mixture of CO_2 and C_2H_6. First of all, even in the normal gravitational field, the concentration gradients dx/dz of the mixture exhibit a change of sign depending on the bulk concentration of the mixture relative to $\langle x\rangle_{caz}$. They assume positive values when $\langle x\rangle = 0.50$ (which is less than $\langle x\rangle_{caz}$) and they assume negative values when $\langle x\rangle = 0.84$ (which is greater than $\langle x\rangle_{caz}$). The gradient becomes virtually zero when $\langle x\rangle = \langle x\rangle_{caz}$. The reversal of the sign has its origin in the reversal of the volatility of CO_2 and C_2H_6. According to the phase diagram of the mixture of CO_2 and C_2H_6, shown in Fig. 5, CO_2 is the more volatile of the two for mixtures with a CO_2 concentration less than that of an azeotropic mixture. On the other hand, C_2H_6 is the more volatile of the two in those with a CO_2 concentration greater than that of an azeotropic mixture. Therefore, for a mixture of $\langle x\rangle = 0.50$, CO_2 is the more volatile component. Even at supercritical temperatures, in the field of gravity it will be present in a higher concentration in the upper part of the cell because that part is the one occupied by the vapor phase when the mixture separates into two phases. For the case of $\langle x\rangle = 0.84$, CO_2 is the less volatile component and is present in a lower concentration in the upper part of the cell.

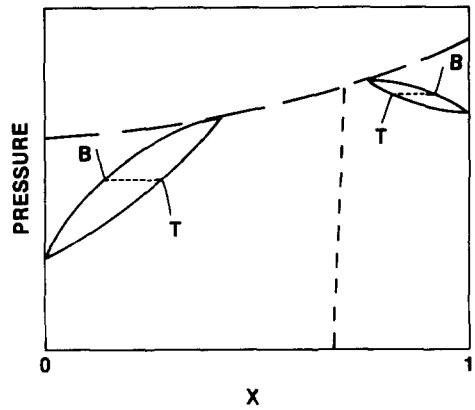

FIG. 5. Schematic representation of gas–liquid equilibrium in the mixture of carbon dioxide and ethane. The critical line is shown as the long-dashed curve and the azeotropic line is shown as the short-dashed line. The phase boundaries at about 20 °C are shown as two loops. The drawing is not to scale. The curved segments terminating at the phase boundaries depict the states of mixtures in a sealed cell in a gravity field in the two-phase region. The top and the bottom of the cell are marked by T and B, respectively. Tie lines are shown as dotted lines. $X = 1$ represents pure CO_2.

For simple fluids near a gas–liquid critical point, the density gradient $d\rho/dz$ diverges according to the power law $|t|^{-\gamma}$ along the critical isochore.[2,3,10] But for binary fluid mixtures near a plait point, Mistura[21] has pointed out that both $d\rho/dz$ and dx/dz diverge according to the same γ power law, except at the critical azeotrope where dx/dz vanishes. Binary liquid mixtures near a consolute point form a special case when the fluids are relatively incompressible. The results of our calculations agree with his prediction and also illustrate the behavior of the secondary contributions to the gradients as the coefficient of the strongest contribution passes through zero at the azeotrope. In the framework of the Leung–Griffiths equation of state, the concentration gradient is expressed in four parts. The first three parts are terms proportional, respectively, to $(\omega_\zeta + B_\zeta\omega_\tau)r^{-\gamma}$, $\theta r^{\beta-1}$, and $r^{-\alpha}$, and the fourth part consists of terms proportional to r with exponents greater than or equal to 0. Here r is the Schofield's distance variable which, along the special paths of critical isochore or critical isopleth, becomes proportional to t. In general, when a critical point is approached ($r \to 0$) the first part diverges strongly and becomes the dominant term resulting in a large gradient, except near a critical azeotrope because $(\omega_\zeta + B_\zeta\omega_\tau)$ vanishes along an azeotropic line, where this coefficient changes sign. This change of sign is responsible for the reversal of sign of dx/dz for $\langle x\rangle = 0.50$ and $\langle x\rangle = 0.84$, as illustrated in Figs. 3(a) and 3(c). For $\langle x\rangle = \langle x\rangle_{caz}$, $(\omega_\zeta + B_\zeta\omega_\tau)$ is so small that the contribution to the concentration gradients comes mostly from the second part which, however, is itself negligibly small in the normal gravitational field so that x does not vary with height, as shown in Fig. 3(b). This second part is something of a curiosity; although $r^{\beta-1}$ diverges more strongly than the third

part, $r^{-\alpha}$, the second part as a whole does not diverge because the multiplicative factor θ is zero at a critical point. Whereas the first part is an even function of θ, the second part is an odd one which results in a characteristically different feature as θ changes sign when ρ goes from greater than to less than ρ_c. The weakly diverging third part is found to be negligible under conditions that are accessible experimentally. Simply speaking, the only significant contribution to dx/dz in normal gravity comes from the first part which exhibits the strong γ divergence.

We can, however, amplify the effects of each part by increasing the gravitational acceleration. For instance, when $\langle x\rangle = \langle x\rangle_{caz}$, the dominant contribution from the second part can be made to manifest itself in a high gravitational field. As shown in Fig. 4(b), the bracket-like bend in the concentration profile at the center is just such a manifestation. As a matter of fact, in a high gravitational field, the states of the mixture away from the center of the cell are so far removed from the critical point that the first part is no longer dominant. Consequently, all parts except the third become comparable in magnitude resulting in the unusual shapes for the concentration profiles in Figs. 4(a) and 4(c). The interesting behavior of the concentration profiles is related to the presence of an azeotropic line. In a mixture of He^3 and He^4, subjected to a large gravitational force, the predicted density and concentration profiles exhibit the same general features as in the case of a normal gravitational field.

Given the condition that $M_1 > M_2$ such as is the case for the mixture of carbon dioxide and ethane, Eq. (31) seems to mandate that the top (or bottom) of the cell should contain pure ethane (or carbon dioxide) when $gz \to \infty$ (or $-\infty$) because $\zeta \to 1$ (or 0) at that limit. This notion is consistent with the physical intuition for the limit $gz \to \infty$ where the ideal gas equation of state will prevail but it is not necessarily correct for the limit $gz \to -\infty$, in which all fluids become close-packed liquids. The concentration profiles calculated for a large gravitational field shown in Fig. 4 indicate, misleadingly, increasing CO_2 concentrations not only towards the bottom, but also towards the top of the cell. The gravitational acceleration of 2×10^5 times g, however, does not sufficiently approximate the limiting case of $|gz| \to \infty$, but at higher gravitational acceleration the empirical limit of validity of the Schofield linear model will be exceeded. If, for these limiting states far removed from criticality we choose a van der Waals equation of state for the mixture[27,28] we can show that if $M_1 > M_2$, then x will approach the value zero (pure ethane) as $gz \to \infty$. But for the limiting case of $gz \to -\infty$, x will approach the value 1 if $M_1/b_1 > M_2/b_2$, where b_1 and b_2 are the excluded volume parameters, respectively, of carbon dioxide and ethane. The first part of the conclusion is consistent with the notion that the ideal gas equation will prevail as $gz \to \infty$ because $\rho \to 0$ and consequently gases of lighter molecular weight float to the top. The second part states that when the fluids are as dense as liquids, the denser one sinks. For the mixture of carbon dioxide and ethane, the ratio of molecular weight to excluded volume parameter is indeed larger for CO_2 than for C_2H_6 and consequently the former must eventually sink. The equations relevant to the discussions can be found in the Appendix.

VI. CRITIQUE

For our applications, the equation of state as presented in Sec. II is not without deficiencies. One of the most serious drawbacks is the use of the Schofield linear model. First of all, its applicability is restricted to a small range around a critical point. More seriously, it assumes that the coexistence curve of a pure fluid is symmetric in density with respect to ρ_c. Generally speaking, the assumption is not correct for real fluids near a critical point. Helium-3 and helium-4 are found to be exceptions; the two pure fluids have nearly symmetric coexistence curves and the Leung–Griffiths thermodynamic potential describes the known physical properties of the mixture adequately.[23,29] Thus we expect the calculated gravity effects in this mixture to be realistic. In the case of the mixture of carbon dioxide and ethane, the lack of skewness in the model coexistence curve with respect to density may prove to be a significant shortcoming. The deficiency could be remedied, in principle, by the mixing of variables and the introduction of correction-to-scaling terms as in the case of simple fluids.[30] However, this complicated procedure has yet to be worked out for mixtures. Moldover *et al.* introduced asymmetry into the thermodynamic potential of the Leung–Griffiths type by a simpler approach[31,32] for a number of mixtures including the mixture of CO_2 and C_2H_6. But the use of the thermodynamic potential has been restricted to the two-phase region.

In spite of the deficiencies in the equation of state, we believe that the general features of the density and concentration gradients will not be essentially modified when an improved equation is used, because these features are induced by the strong critical anomalies which have been properly incorporated in the equation.

In our calculations, we assume that the mixture is in local equilibrium everywhere in the cell. This assumption ceases to be valid very close to a critical point because of nonlocal effects when the correlation length of critical fluctuations becomes comparable to the range of height over which the densities vary appreciably.[33] In this context, lengthening of the sample cell is not equivalent to increasing the gravitational acceleration. However, the nonlocal effects are significant only when t is about 10^{-6} or less, therefore, for most cases, such as our calculations, one can neglect the nonlocal effects without serious consequences.

VII. SUMMARY

Using a nonclassical equation of state of the mixtures of He^3 and He^4 and of CO_2 and C_2H_6 near a critical line, we have calculated the profiles of density and concentration in a sealed cell of a finite height. The gravity effect is found to be larger in the mixture of He^3 and He^4 than in that of CO_2 and C_2H_6. The temperature at which a mixture first separates into two phases is different from the critical temperature determined by the bulk parameters. The gravity-induced density profiles of

mixtures are very insensitive to the bulk concentration of the mixtures and show the same features as those in simple fluids. On the other hand, the concentration profiles show a variety of features from one mixture to another. For instance, the concentration gradient virtually vanishes in the critical azeotropic mixture of CO_2 and C_2H_6. For mixtures with bulk CO_2 concentration larger than that of the critical azeotropic mixture, the concentration profiles show an increase in CO_2 with increasing height whereas for the mixtures with bulk CO_2 concentration less than that of the critical azeotropic mixture, the profiles show a decrease in CO_2 with increasing height. But if the cell is infinitely long or the gravitational field is infinitely strong, the ideal gas equation and sedimentation effect shall prevail, respectively, at the top and the bottom of the cell causing ethane to float to the top and carbon dioxide to sink towards the bottom.

We have also shown that the location of the meniscus at the phase transition is not affected by gravity in any significant way; the meniscus motion in mixtures of He^3 and He^4 observed by Miura *et al.* cannot be explained by the gravity effect alone based on the analysis using the Leung–Griffiths equation of state.

ACKNOWLEDGMENTS

We wish to thank Professor H. Meyer and Professor R. L. Scott, Dr. G. Morrison, and Dr. M. R. Moldover for valuable discussions, and Mr. D. Diller for careful reading of the manuscript. Professor Meyer provided us with experimental information prior to publication.

APPENDIX

The van der Waals equation for a mixture can be written as

$$Bp = 1/(v-b) - Ba/v^2 , \tag{A1}$$

where v is the molar volume. The attractive parameter a and the excluded volume parameter b of the mixture are expressed in terms of their respective component parameters by the following mixing rules:

$$a = x^2 a_1 + 2x(1-x)a_{12} + (1-x)^2 a_2 \tag{A2}$$

and

$$b = xb_1 + (1-x)b_2 , \tag{A3}$$

where a_{12} is the attractive parameter between the molecules of components 1 and 2. The parameters a_1, a_2, b_1, and b_2 here should not be confused with those in Sec. II. The explicit form of a_{12} is not required for the following discussion but explicit in Eq. (A3) is the assumption that the excluded volume of a mixture is the average of that of the components weighted according to the respective concentrations. From Eq. (A1), one can show that [27,28]

$$B\mu_i = \ln x_i - \ln[(v-b)/v_B] + b_i/(v-b) - 2BH_i/v , \quad \text{for } i = 1 \text{ and } 2 , \tag{A4}$$

where

$$x_1 = x , \quad x_2 = (1-x) ,$$

$$H_1 = a_1 x + a_{12}(1-x) , \quad H_2 = a_{12} x + a_2(1-x) ,$$

and v_B is a constant with the dimension of volume. Introducing the gravitational field into Eq. (A4) we obtain

$$U_1 - BM_1 gz = \ln x - \ln[(v-b)/v_B] + b_1/(v-b) - 2BH_1/v \tag{A5}$$

and

$$U_2 - BM_2 gz = \ln(1-x) - \ln[(v-b)/v_B] + b_2/(v-b) - 2BH_2/v , \tag{A6}$$

where U_1 and U_2 are the constants of integration which are determined by the bulk parameters $\langle x \rangle$ and $\langle v \rangle$, the latter being an inverse of $\langle \rho \rangle$. Eliminating z by combining Eqs. (A5) and (A6), we obtain

$$M_2 \ln x - M_1 \ln(1-x) - (M_2 - M_1)\ln[(v-b)/v_B] + (M_2/b_2 - M_1/b_1)b_1 b_2/(v-b) - 2B(M_2 H_1 - M_1 H_2)/v - (M_2 U_1 - M_1 U_2) = 0 . \tag{A7}$$

From Eqs. (A5)–(A7) we can conclude that $x \to 0$ (or 1) if M_2 is less than or greater than M_1 at the limit $gz \to +\infty$ and $x \to 0$ (or 1) if M_2/b_2 is greater than or less than M_1/b_1 at the limit $gz \to -\infty$. For the mixture of CO_2 and C_2H_6 we have $M_1 \simeq 44$ g/mol and $M_2 \simeq 30$ g/mol, while from the respective critical volumes we estimate $b_1 \simeq 0.031$ ℓ/mol, and $b_2 \simeq 0.048$ ℓ/mol; therefore CO_2 should sink to the bottom while C_2H_6 floats to the top.

[1] G. Gouy, C. R. Acad. Sci. 115, 720 (1892).
[2] P. C. Hohenberg and M. Barmatz, Phys. Rev. A 6, 289 (1972).
[3] M. R. Moldover, J. V. Sengers, R. W. Gammon, and R. J. Hocken, Rev. Mod. Phys. 51, 79 (1979).
[4] O. Splittorff and B. N. Miller, Phys. Rev. A 9, 550 (1974).
[5] D. M. Kim, D. L. Henry, and R. Kobayashi, Phys. Rev. A 10, 1808 (1974).
[6] H. K. Leung and B. N. Miller, Phys. Rev. A 12, 2162 (1975).
[7] H. K. Leung and B. N. Miller, Phys. Rev. A 16, 406 (1977).
[8] S. C. Hornbostel and B. N. Miller, Phys. Rev. A 20, 1728 (1979).
[9] E. H. W. Schmidt, in *Critical Phenomena*, edited by M. S. Green and J. V. Sengers, Natl. Bur. Stand. 273 (U.S. GPO, Washington, D.C., 1966), p. 13.
[10] R. J. Hocken and M. R. Moldover, Phys. Rev. Lett. 37, 29 (1976).
[11] H. L. Lorentzen and B. B. Hansen, in *Critical Phenomena*, edited by M. S. Green and J. V. Sengers, Natl. Bur. Stand. 273 (U.S. GPO, Washington, D.C., 1966), p. 213.
[12] A. A. Fannin, Jr. and C. M. Knobler, Chem. Phys. Lett. 25, 92 (1974).
[13] S. C. Greer, T. E. Block, and C. M. Knobler, Phys. Rev. Lett. 34, 250 (1975).
[14] G. Maisano, P. Migliardo, and F. Wanderlingh, J. Phys. A: Math. Nucl. Gen. 9, 2149 (1976).
[15] T. E. Block, E. Dickinson, C. M. Knobler, V. N. Schumaker, and R. L. Scott, J. Chem. Phys. 66, 3786 (1977).
[16] R. Salinas, H. S. Huang, and J. Winnick, in *Equations of State in Engineering and Research*, edited by K. C. Chao and R. L. Robinson, Jr. (American Chemical Society, Washington, D.C., 1979), Chap. 15, p. 271.
[17] C. Pittman, T. Doiron, and H. Meyer, Phys. Rev. B 20, 3678 (1979).
[18] J. P. Kuenen, Commun. Phys. Lab. Leiden, 17, 1 (1895).

[19]R. F. Chang and T. Doiron, *Proceedings of the Eighth Symposium on Thermophysical Properties, Vol. 1: Thermophysical Properties of Fluids*, edited by J. V. Sengers (American Society of Mechanical Engineers, New York, 1981), p. 458.
[20]Y. Miura, H. Meyer, and A. J. Ikushima, Phys. Lett. 91, 309 (1982).
[21]L. Mistura, J. Chem. Phys. 55, 2375 (1971).
[22]S. P. Malyshenko and V. I. Mika, Teplofiz. Vys. Temp. 12, 735 (1974).
[23]S. S. Leung and R. B. Griffiths, Phys. Rev. A 8, 2670 (1973).
[24]T. Doiron and R. F. Chang (to be published).
[25]P. Schofield, Phys. Rev. Lett. 22, 606 (1969).
[26]J. V. Sengers and J. M. H. Levelt Sengers, in *Progress in Liquid Physics*, edited by C. A. Croxton (Wiley, Chichester, United Kingdom, 1978), Chap. 4, p. 103.
[27]P. H. van Konynenburg and R. L. Scott, Philos. Trans. R. Soc. London 298, 495 (1980).
[28]J. A. Gualtieri, J. M. Kincaid, and G. Morrison, J. Chem. Phys. 77, 521 (1982).
[29]T. Doiron, R. P. Behringer, and H. Meyer, J. Low Temp. Phys. 24, 345 (1976).
[30]J. M. H. Levelt Sengers, B. Kamgar-Parsi, and J. V. Sengers, J. Phys. Chem. Ref. Data 12, 1 (1983).
[31]M. R. Moldover and J. S. Gallagher, AIChE J. 24, 267 (1978).
[32]J. C. Rainwater and M. R. Moldover, in *Chemical Engineering at Supercritical Fluid Conditions*, edited by M. E. Paulaitis, J. M. L. Penninger, R. D. Gray, Jr., and P. Davidson (Ann Arbor Science, Ann Arbor, 1983), Chap. 10, p. 199.
[33]J. V. Sengers and J. M. J. van Leeuwen, Physica A 116, 345 (1982).